

See discussions, stats, and author profiles for this publication at: <https://www.researchgate.net/publication/7247513>

Differential cell adhesion to vocal fold extracellular matrix constituents

Article in *Matrix Biology* · June 2006

DOI: 10.1016/j.matbio.2006.01.004 · Source: PubMed

CITATIONS

12

READS

29

4 authors, including:



Erin Ostrem

uw library

1 PUBLICATION 12 CITATIONS

[SEE PROFILE](#)



Ingo R Titze

University of Utah

424 PUBLICATIONS 21,266 CITATIONS

[SEE PROFILE](#)

Some of the authors of this publication are also working on these related projects:



An Optimizer-Simulator for Phonosurgery [View project](#)



Voice disorders and assessment [View project](#)

Differential cell adhesion to vocal fold extracellular matrix constituents

Tannin J. Fuja^{a,*}, Erin M. Ostrem^a, Megan N. Probst-Fuja^a, Ingo R. Titze^{a,b}

^a National Center for Voice and Speech, Department of Speech Pathology and Audiology, The University of Iowa, Iowa City, IA 52242, USA

^b National Center for Voice and Speech, The Denver Center for the Performing Arts, Denver, CO 80204, USA

Received 4 November 2005; received in revised form 10 January 2006; accepted 10 January 2006

Abstract

The human vocal folds are a complex layering of cells and extracellular matrix. Vocal fold extracellular matrix uniquely contributes to the biomechanical viscoelasticity required for human phonation. We investigated the adhesion of vocal fold stellate cells, a novel cell type first cultured by our laboratory, and fibroblasts to eight vocal fold extracellular matrix components: elastin, decorin, fibronectin, hyaluronic acid, laminin and collagen types I, III and IV. Our data demonstrate that these cells adhere differentially to said substrates at 5 to 120 min. Cells were treated with hyaluronidase and Y-27632, a p160ROCK-specific inhibitor, to test the role of pericellular hyaluronan and Rho-ROCK activation in early and mature adhesion. Reduced adhesion resulted; greater inhibition of fibroblast adhesion was observed. We modulated the fibronectin affinity exhibited by both cell types using Nimesulide, an inhibitor of fibronectin integrin receptors $\alpha 5\beta 1$ and $\alpha v\beta 3$. Our results are important in understanding vocal fold pathologies, wound healing, scarring, and in developing an accurate organotypic model of the vocal folds.

© 2006 Elsevier B.V./International Society of Matrix Biology. All rights reserved.

Keywords: Adhesion; Extracellular matrix; Stellate cell; Rho A; Integrin; Actin; Vocal cord

1. Introduction

The human vocal folds are a unique structure consisting of thin outer epithelia, a lamina propria (LP) rich in extracellular matrix (ECM) and the vocalis muscle. A number of proteoglycans have been identified within the ECM of the vocal folds including: 1) small, interstitial matrix proteoglycans such as decorin and fibromodulin, and 2) a large, aggregating proteoglycan called versican (Pawlak et al., 1996). They appear to aid in the regulation of the other matrix proteins in the LP (Gray et al., 1999b). Only one glycosaminoglycan, hyaluronic acid (HA), has been identified in the vocal fold LP. It is found abundantly throughout the LP, but is particularly abundant in the superficial layer. The glycoprotein fibronectin has been found ubiquitously

throughout the vocal fold LP. The function of fibronectin remains largely unknown but it is thought to be important in cell adhesion. Various collagen types have been identified in the LP and BMZ of the vocal folds. However, collagen types I, III, and IV have been consistently identified in various studies from several laboratories. Collagen type IV is principally found in the BMZ, and collagen type III is the predominant collagen in the LP. Collagen fibers are most dense in the deep layer of the LP, but are also found to lesser extents in the other layers. Collagen fibers have been shown to align their orientation to withstand longitudinal stress associated with vocal fold oscillation (Gray et al., 2000, 1993). Remarkably, the glyco-matrix proteoglycans also have a layered orientation similar to fibrous proteins in LP (Gray et al., 1999b). While collagen is critical in bearing stress and resisting deformation during phonation, elastin allows tissue to return to its original shape following deformation (Gray, 2000). The intermediate layer of the LP is characterized by extensive mature elastin fibers also found to lesser extents in the deep layer.

In addition to ECM, the LP contains scattered fibroblasts at varied cellular densities. These fibroblasts were thought to be primarily responsible for maintaining vocal ECM homeostasis and regulating injury response. Recently, however, our

Abbreviations: LP, lamina propria; BMZ, basement membrane zone; HA, hyaluronic acid; VFSC, vocal fold stellate cell; TF, tracheal fibroblast; FX, focal complexes; FA, focal adhesions; FB, fibrillar adhesions.

* Corresponding author. National Center for Voice and Speech, Department of Speech Pathology and Audiology, 330 Wendell Johnson Speech and Hearing Center, University of Iowa, Iowa City, Iowa 52242, USA. Tel.: +1 319 335 6591; fax: +1 319 335 6603.

E-mail address: tannin-fuja@uiowa.edu (T.J. Fuja).

laboratory isolated and cultured a new type of cell called a vocal fold stellate cell (VFSC), identified in the macula flava of the vocal ligament. The bending stresses on the vocal folds associated with phonation are the greatest in the region of the macula flava (Titze and Hunter, 2004). The ECM of the macula flava is composed of collagenous, reticular, and elastic fibers running in various directions. HA is found in the inter-fibrillary spaces of the macula flava (Sato et al., 2003a). The maculae flavae not only impact phonation, but also development, growth, and aging of the vocal folds (Sato and Hirano, 1995). We have demonstrated that VFSCs undergo culture-induced activation or transdifferentiation (Fuja et al., 2005, 2006). Similar to activated pancreatic and hepatic stellate cells, activated VFSCs lose intracellular lipid droplets and retinol metabolite stores, proliferate rapidly, secrete large amounts of ECM and demonstrate a myofibroblastic phenotype (Jaster, 2004; Geerts, 2004). Quiescent VFSCs possess intracellular lipid droplets containing vitamin A metabolites. Stellate cell activation in the liver and pancreas has been shown to play a central role in fibrogenesis, ECM remodeling and wound healing. It is currently not known what role VFSCs play in normal vocal fold development, vocal aging or in pathological conditions such as laryngeal fibrosis or scarring.

Knowledge of the interaction between the cellular and ECM components of the LP will be important in understanding vocal fold wound healing, fibrogenic pathologies and scarring, response to phonotrauma and laryngeal cancer. For example, adhesion between hepatic stellate cells and ECM regulates fibrogenesis (Sato et al., 2003b). Cell adhesion is an active molecular process. Published data suggest that within a few seconds of contact between a cell and a surface HA begins to mediate adhesion. Within the next tens of seconds to minutes, the HA mediated adhesions are replaced by integrin-containing contacts.

The cell adhesion processes of VFSCs or laryngeal fibroblasts to vocal fold ECM are unknown. We investigated cell adhesion between vocal fold ECM components and VFSCs or fibroblasts. Our results are important in conceptualizing vocal fold wound healing, response to vibrational stress, and in the development of accurate organotypic models of the LP.

2. Results

2.1. Adhesion of untreated cells

VFSCs and tracheal fibroblasts (TFs) were allowed to adhere to nine different surfaces (collagen types I, III, IV, HA, decorin, laminin, elastin and an uncoated control) for 5, 10, 15, 20, 30 or 120 min. Fig. 1 summarizes the results of these experiments. Overall the VFSCs and TFs adhered best to fibronectin followed by elastin and the uncoated surface. Both cell types demonstrated better adhesion to fibronectin at the early time points than the other ECM coatings. The adhesive affinities of VFSCs and TFs to the various ECM coatings were compared at each time point. On the uncoated surface the VFSCs were significantly more adherent than the TFs at 5 min ($p=0.0065$), 10 min ($p=0.0056$), 15 min ($p=0.0079$), 20 min ($p=0.0104$) and 30 min ($p=0.0121$). There was no significant difference in adhesion

to an uncoated surface between the two cell types after 120 min. The VFSCs were significantly more adherent to fibronectin than the TFs at 5 min ($p=0.0124$) and 10 min ($p=0.0316$), but there were no significant differences in adhesion to fibronectin after that time. There were no significant differences in the number of VFSCs or TFs adhering to HA which in general was low. TFs exhibited a significantly higher affinity for collagen type III than the VFSCs at 15 min ($p=0.0370$), 20 min ($p=0.0336$) and collagen type I at 30 min ($p=0.0156$). Overall, both cell types adhered to laminin the least. The VFSCs and TFs demonstrated intermediate adherence to decorin and the collagen types examined.

We compared the adherence of VFSCs and TFs on an uncoated surface to their adherence on each of the eight ECM coated surfaces. The VFSCs and TFs adhered significantly better to fibronectin at 5 min (VFSC $p=0.0035$; TF $p=0.0031$), 10 min (VFSC $p=0.0052$; TF $p=0.0033$), 15 min (VFSC $p=0.0054$; TF $p=0.0034$), 20 min (VFSC $p=0.0056$; TF $p=0.0036$) and 30 min (VFSC $p=0.0057$; TF $p=0.0035$). The TFs but not the VFSCs adhered significantly better to the HA at 5 min ($p=0.0242$), 10 min ($p=0.0362$) and 15 min ($p=0.0350$). The VFSCs adhered significantly better to the uncoated surface compared to HA at 20 min ($p=0.0304$) and both cell types adhered better to the uncoated surface at 120 min (VFSC $p=0.0364$; TF $p=0.0112$). The TFs adhered better to collagen type III compared to the uncoated surface at 5 min ($p=0.0124$), 10 min ($p=0.0019$), 15 min ($p=0.0241$), 20 min ($p=0.0282$) and 30 min ($p=0.0350$). In contrast, the VFSCs adhered better to the uncoated surface than to collagen type III at 15 min ($p=0.0285$), and 20 min ($p=0.0429$). VFSCs adhered less to collagen type IV and laminin than the uncoated surface. This difference was significant at 5 min (collagen IV $p=0.0091$; laminin $p=0.0036$), 10 min (collagen IV $p=0.0201$; decorin $p=0.0048$; laminin $p=0.0126$), 15 min (collagen IV $p=0.0201$; decorin $p=0.0101$; laminin $p=0.0049$), 20 min (collagen type IV $p=0.0208$; decorin $p=0.0156$; laminin $p=0.0185$), 30 min (decorin $p=0.0082$; laminin $p=0.0079$) and 120 min (decorin $p=0.0181$; laminin $p=0.0294$). Comparatively, TFs adhered equivalently to collagen IV, decorin and laminin at 5 and 10 min. Significantly stronger adhesion to an uncoated surface than to certain ECM substrates was observed at 15 min (decorin $p=0.0028$; laminin $p=0.0099$), 20 min (decorin $p=0.0472$; laminin $p=0.0048$), 30 min (collagen IV $p=0.0365$; decorin $p=0.0094$; laminin $p=0.0338$) and 120 min (decorin $p=0.0185$; laminin $p=0.0027$). The only significant difference between VFSC or TF adhesion to collagen type I compared to an uncoated surface was found at 15 min (VFSC $p=0.0302$) where the VFSCs adhered less well to collagen type I and at 30 min (TF $p=0.0014$) where the TFs adhered better to collagen type I. Little significant difference in adhesion to elastin compared to an uncoated surface was found except at 10 min (TF $p=0.0061$) and 20 min (VFSC $p=0.0412$) where in both cases the cells adhered better to elastin.

We then analyzed the differences in adhesion over the time intervals studied to test for significant differences. As reported in Fig. 1, the number of cells adhering to the various surfaces always increased with incubation time prior to washing.

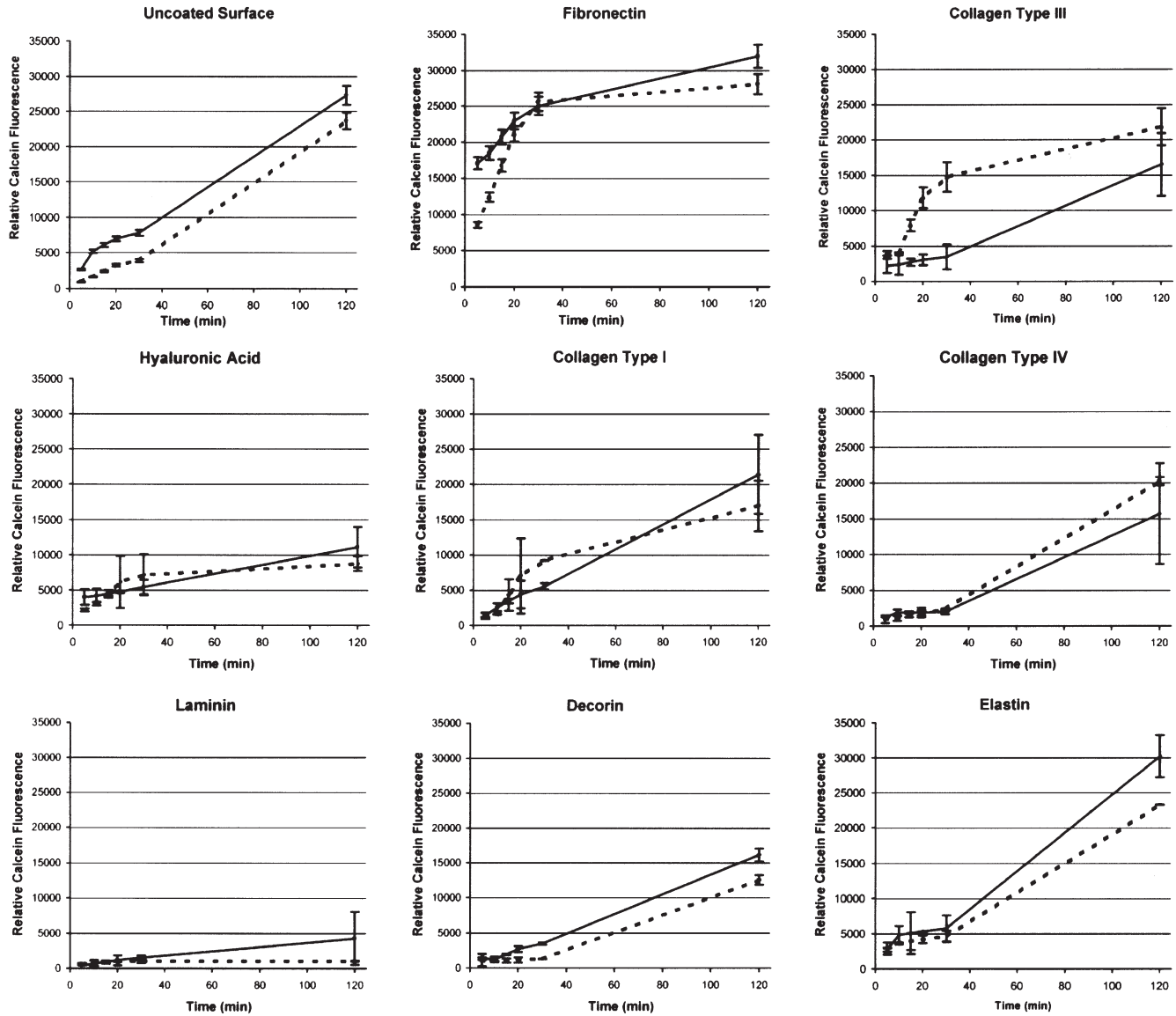


Fig. 1. Adhesion of untreated VFSCs and TFs to ECM components of the vocal fold mucosa. These graphs present relative calcein fluorescence over the time intervals tested from the VFSCs (solid line) and the TFs (dashed line) adhering to each of the major vocal fold ECM coated and the uncoated control surfaces. Error bars represent \pm s.e.m. ($n=4$ using 5×10^4 cells per well).

Statistically significant differences in the number of TFs adhering after 120 min compared to 5 min were found for all surfaces tested except laminin (no coat $p=0.0188$; fibronectin $p=0.0056$; HA $p=0.0257$; collagen type I $p=0.0494$; collagen type III $p=0.0219$; collagen type IV $p=0.0017$; decorin $p=0.0073$; elastin $p=0.0018$). In contrast, significant differences in VFSC adhesion at 120 min compared to 5 min were found for the uncoated surface ($p=0.0097$), fibronectin ($p=0.0145$), decorin ($p=0.0056$) and elastin ($p=0.0018$). The only statistically significant increase in cell adhesion between 5 to 10 min was found in the TFs on fibronectin ($p=0.0371$). The significant increase in adhesion for VFSCs on fibronectin occurs earlier than 5 min. The increase in the number of VFSCs adhering to the various surfaces occurs at a constant rate such that no statistically significant differences were found from 5 to 30 min, but collectively over the entire experiment changes in VFSC adhesion are statistically significant. TF adherence does

increase significantly from 10 to 15 min on collagen type III ($p=0.0465$) and on an uncoated surface ($p=0.0003$). From 30 to 120 min a significant increase in TF adhesion is observed on elastin ($p=0.0019$), decorin ($p=0.0074$), collagen type IV ($p=0.0013$) and on an uncoated surface ($p=0.0283$). During that same time interval a significant increase in VFSC adhesion is observed on elastin ($p=0.0279$), decorin ($p=0.0029$) and on an uncoated surface ($p=0.0073$).

We confirmed the ability of VFSCs and TFs to grow successfully to confluence on each surface over time. The morphology of the VFSCs and TFs grown on the various substrates was examined using fluorescence confocal microscopy. VFSCs and TFs were grown on Desag borosilicate growth coverglass (Fisher Scientific; Pittsburgh, PA) coated with the various substrates for approximately 72 h, acetone-fixed, and labeled with TRITC-phalloidin (Molecular Probes; Eugene, OR) to examine the effect of the various ECM components on the

formation of organized actin stress fibers. Our results demonstrate that every surface tested supported cell growth and to varying extents the formation of mature, elongated F-actin fibers with an aligned orientation. Fig. 2 presents representative fluorescence confocal micrographs of the VFSCs and TFs grown on the vocal fold ECM substrates studied.

2.2. Adhesion of hyaluronidase treated cells

The pericellular HA coat of some cells has been suggested to be important in the initial stages of cell adhesion (Zimmerman et al., 2002). To test its role in VFSC and TF adhesion, these cells were treated with hyaluronidase and incubated on the nine

different surfaces for 5, 10 and 15 min. Hyaluronidase randomly cleaves β -*N*-acetylhexosamine-[1 \rightarrow 4] glycosidic bonds in HA, chondroitin, and chondroitin sulfates. Fig. 3 summarizes the results of these experiments. Hyaluronidase treatment reduced the number of adherent cells on every surface. The effect of this digestion was most noticeable on those cells incubated on all of the collagens tested, laminin, and decorin. Overall TF adhesion was more affected by the treatment than the VFSCs. We compared the adherence of the treated VFSCs to the TFs at every time point on each of the nine surfaces. In all cases, the hyaluronidase treated VFSCs adhered better than the treated TFs. This difference was statistically significant at 5 min (uncoated $p=0.0056$; fibronectin $p=0.0440$; HA $p=0.0059$;

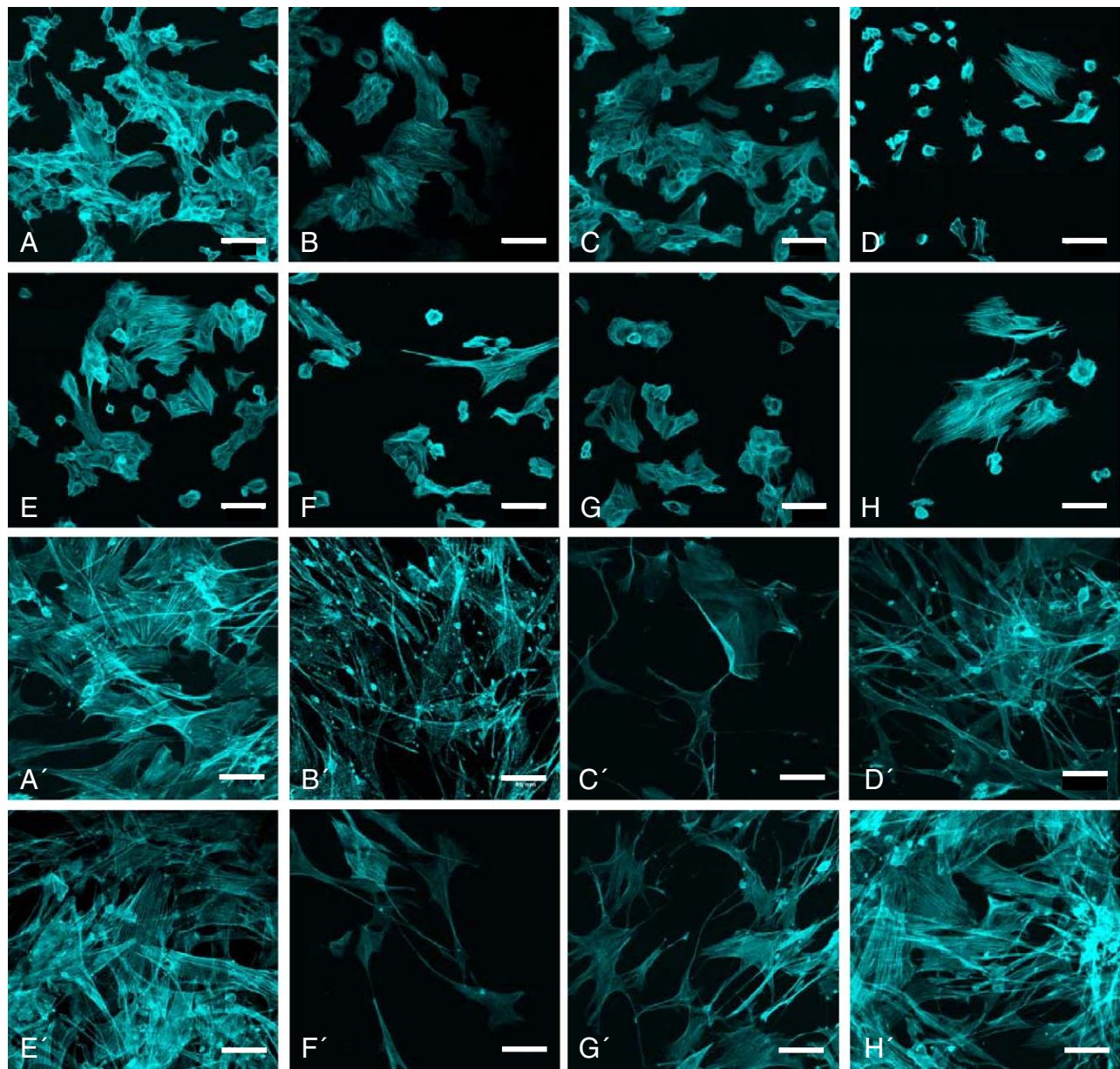


Fig. 2. Fluorescence confocal micrographs of VFSCs and TFs grown on various ECM substrates. To determine the ability of VFSCs to grow on each substrate and form mature, elongated F-actin fibers with aligned orientation, these cells were stained with TRITC-phalloidin and imaged using fluorescence laser-scanning confocal microscopy. The micrographs present representative images of VFSCs (A–H) and TFs (A'–H') grown on: HA (A, A'), fibronectin (B, B'), collagen type IV (C, C'), collagen type I (D, D'), elastin (E, E'), decorin (F, F'), collagen type III (G, G'), and laminin (H, H'). The scale bar represents 55 nm.

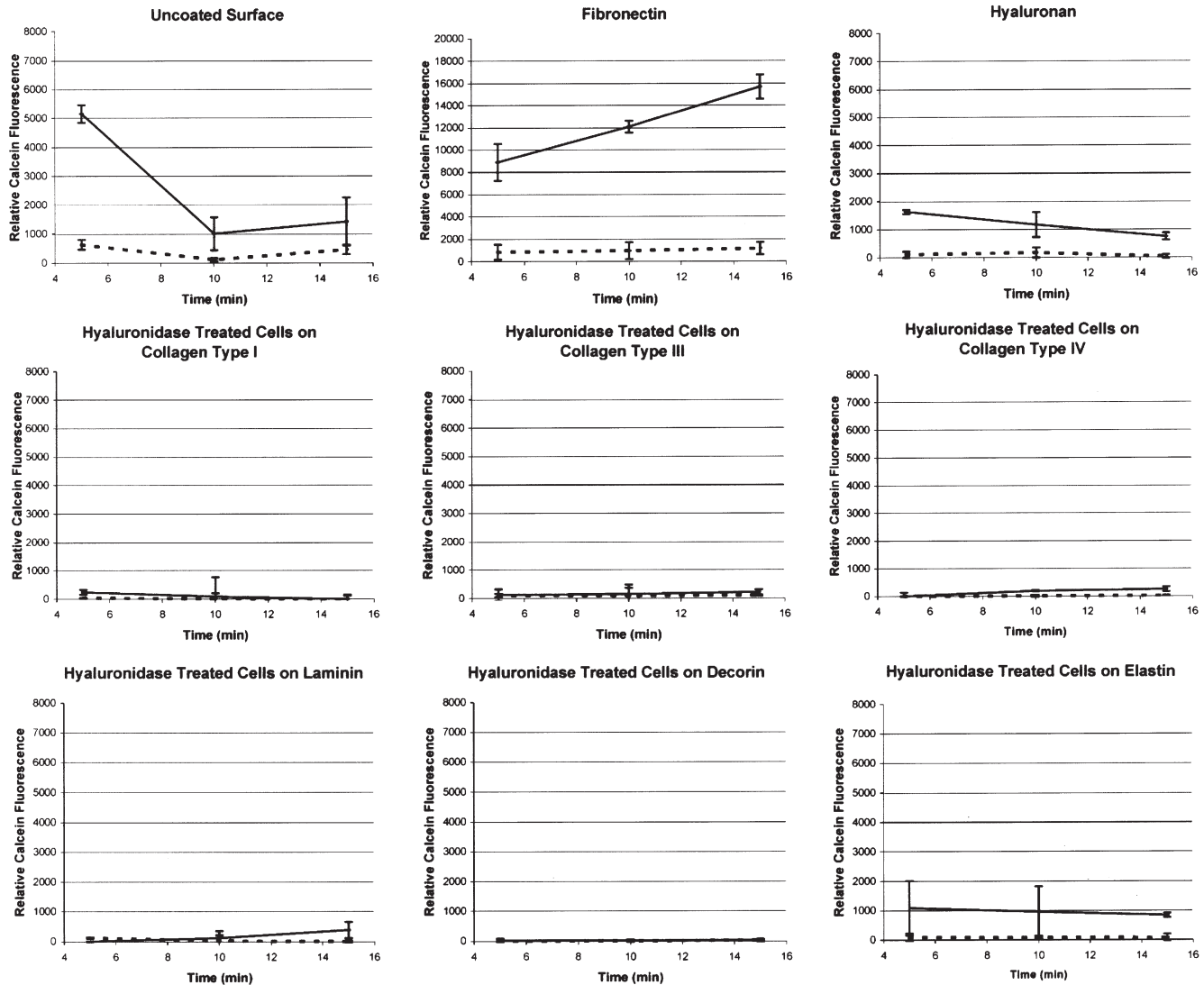


Fig. 3. Adhesion of hyaluronidase treated VFSCs and TFs. Here is the summary of the adhesion of VFSCs (solid line) and TFs (dashed line) following hyaluronidase treatment. The relative calcein fluorescence from the cells adhering at 5, 10, and 15 min is presented for each of the surfaces tested. Note that the y-axis is scaled greater for fibronectin. Error bars represent \pm s.e.m. ($n=4$ using 5×10^4 cells per well).

collagen type I $p=0.0467$), 10 min (fibronectin $p=0.0065$; collagen IV $p=0.0092$), and 15 min (fibronectin $p=0.0069$; HA $p=0.0261$; collagen IV $p=0.0339$; elastin $p=0.2390$). Interestingly, while hyaluronidase treatment did reduce the number of cells adhering to fibronectin, the effect was much less pronounced than on any other surface tested.

At 5 min, the hyaluronidase treated VFSCs adhered significantly better to an uncoated surface than to all other surfaces tested except fibronectin and elastin (HA $p=0.0079$; collagen type I $p=0.0042$; collagen type III $p=0.0052$; collagen type IV $p=0.0168$; laminin $p=0.0035$; decorin $p=0.0034$). At 5 min, the hyaluronidase treated TFs adhered equally poor to an uncoated surface as to the ECM coated surfaces. Only hyaluronidase treated TF adherence to collagen IV at 5 min was less than to an uncoated surface with marginal significance ($p=0.0470$). At 10 min the hyaluronidase treated VFSCs adhered significantly better to fibronectin than an uncoated surface ($p=0.0048$). This significant difference was maintained at 15 min ($p=0.0092$). No

other significant differences were found between hyaluronidase treated VFSCs and TFs grown on ECM coated surfaces compared to an uncoated surface. Adhesion of both types of treated cells was reduced compared to the adhesion of both types of untreated cells.

Remarkably, the number of adherent cells did not increase significantly with time for either the TFs or VFSCs on any of the surfaces tested. The number of adherent hyaluronidase treated VFSCs significantly decreased on uncoated surfaces from 5 to 10 min ($p=0.0234$). However, only treated VFSCs on HA ($p=0.0248$) and treated TFs on laminin ($p=0.0499$) demonstrated a significant decrease in the number of adherent cells over the entire time course of the experiment.

2.3. p160ROCK/ROK inhibited cell adhesion

A family of Rho-associated serine/threonine kinase isoenzymes called p160ROCK and ROK α /Rho-kinase/ROCK-II

comprise a class of RhoA effectors prominent in the regulation of cytoskeletal organization, focal adhesions and stress fibers (Masamune et al., 2003). Rho kinase also regulates contraction, migration, proliferation and modulates the cell morphology of hepatic stellate cells (Ikeda et al., 2003; Burgstaller and Gimona, 2004). To test the role of RhoA activation in the adhesion of VFSCs and TFs to the various ECM surfaces, these cells were treated with Y-27632 a specific inhibitor of the ROCK/ROK family of protein kinases. Y-27632 has also been proven to inhibit hepatic stellate cell activation (Murata et al., 2001; Kawada et al., 1999). Given that RhoA activation plays a role in later maturation of focal adhesions, Y-27632 treated cells were incubated on the various surfaces for 20, 30 and 120 min. The results of these experiments are presented in Fig. 4. At these time points, Y-27632 treatment noticeably decreased the number of adherent TFs on all surfaces tested. This treatment to a lesser extent also lowered the number of adherent VFSCs on all surfaces except fibronectin and decorin. We compared the

number of adherent Y-27632 treated VFSCs to TFs on every surface. For every surface, the number of adherent TFs was less than the number of VFSCs. This difference was significant at 20 min (fibronectin $p=0.0022$; collagen type III $p=0.0199$; collagen type IV $p=0.0158$), 30 min (uncoated $p=0.0060$; fibronectin $p=0.0002$; collagen type I $p=0.0024$; collagen type III $p=0.0104$; laminin $p=0.0177$; elastin $p=0.0212$) and 120 min (uncoated $p=0.0050$; fibronectin $p=0.0129$; HA $p=0.0180$; collagen type I $p=0.0344$; laminin $p=0.0122$; decorin $p=0.0031$; elastin $p=0.0036$).

The number of treated TFs and VFSCs adhering to fibronectin compared to treated TFs and VFSCs adhering to an uncoated surface was significantly greater at 20 min (VFSC $p=0.0088$; TF $p=0.0178$), 30 min (VFSC $p=0.0003$; TF $p=0.0339$) and 120 min (VFSC $p=0.0326$; TF $p=0.0336$). Fibronectin was the only ECM coating to which the Y-27632 treated VFSCs and TFs adhered significantly better than an uncoated surface. Interestingly, at particular time points the

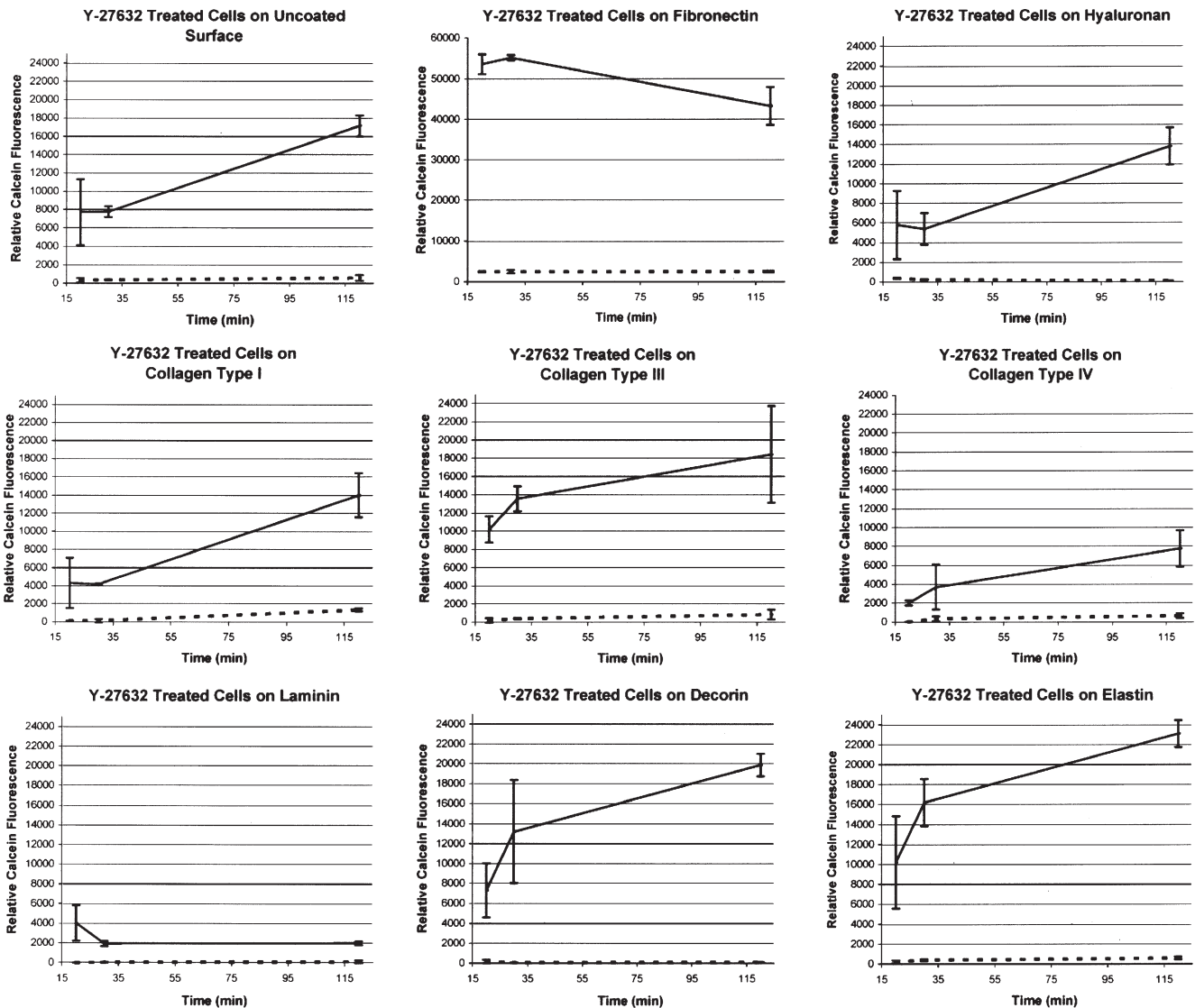


Fig. 4. Adhesion of VFSCs and TFs treated with the p160ROCK inhibitor Y-27632. The results of Y-27632 treatment of VFSCs (solid line) and TFs (dashed line) on cell adhesion to each of the tested surfaces are presented. Note that the y-axis is scaled greater for fibronectin. Error bars represent \pm s.e.m. ($n=4$ using 5×10^6 cells per well).

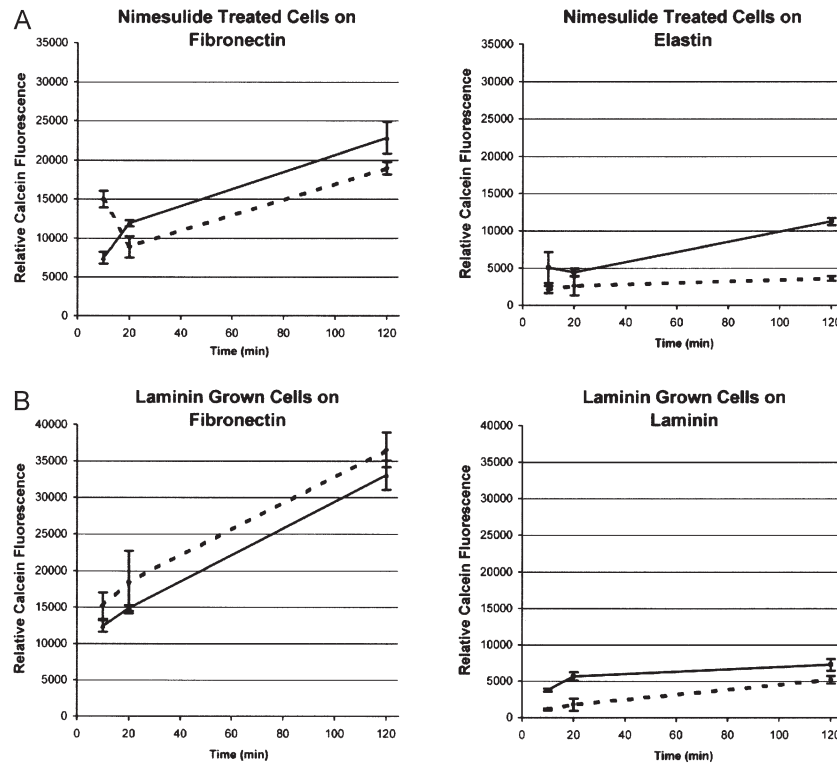


Fig. 5. Modulation of fibronectin adhesion affinity. (A) Altered adherence of VFSCs (solid line) and TFs (dashed line) treated with 250 μ M Nimesulide to fibronectin and elastin coated surfaces. (B) Relative calcein fluorescence of adherent VFSCs (solid line) and TFs (dashed line) grown on laminin to 60% confluence prior to measuring altered adherence of these cells to laminin and fibronectin coated surfaces. In both panels, error bars represent \pm s.e.m. ($n=4$ using 5×10^4 cells per well).

number of Y-27632 treated VFSCs and TFs adhering to some ECM coatings was less than to an uncoated surface. These included VFSCs on collagen type I (30 min $p=0.0263$) and laminin (30 min $p=0.0120$; 120 min $p=0.0058$), and TFs on decorin (30 min $p=0.0291$) and laminin (30 min $p=0.0372$). Overall, the change in the number of adherent Y-27632 treated VFSCs at 20 min compared to 120 min was not significantly different on any surface tested. This same measure on Y-27632 treated TFs demonstrated a significant increase in the number of adherent cells on collagen type I ($p=0.0154$) and a significant decrease in adherent cells on HA ($p=0.0388$).

2.4. Targeting fibronectin affinity cell adhesion

Given the observed high level of untreated cell adhesion to fibronectin and the persistent affinity of hyaluronidase and Y-27632 treated VFSCs for fibronectin, we designed experiments attempting to disrupt this fibronectin affinity. To investigate the role of fibronectin-specific integrin receptors on this affinity, we treated these cells with Nimesulide, a COX-2 inhibitor that also inhibits $\alpha 5\beta 1$ and $\alpha v\beta 3$ integrins. These integrins are the principle fibronectin-binding integrin receptors (Han and Roman, 2005; Milliano and Luxon, 2003; Danen et al., 2002). The ability of Nimesulide-treated cells to adhere to fibronectin and elastin was tested. Data from our experiments, reproduced six times, are reported in Fig. 5A. These results confirm that treatment of VFSCs and TFs with 250 μ M Nimesulide reduces the number of adherent cells on fibronectin by approximately

30% compared to untreated VFSCs and TFs on fibronectin. Interestingly, Nimesulide treatment reduced VFSC and TF adhesion to elastin by nearly 70% compared to untreated cells on elastin with the fibroblasts demonstrating a slightly greater effect.

Next we hypothesized that since the VFSCs and TFs were grown on fibronectin coated surfaces prior to the cell adhesion testing, that these cells may already express important fibronectin receptors prior to the test. Having carefully designed our experimental methods to avoid enzymatic dissociation of the cells, fibronectin-specific receptors would likely remain on the cell surface. To test the effect of cell growth on fibronectin coated surfaces prior to adhesion testing, VFSCs and TFs were passaged using trypsin/EDTA dissociation. This enzymatic digestion was used to strip the cells of surface proteins. The cells were then plated on laminin coated surfaces and grown to 60% confluence prior to repeating the adhesion assay using the laminin-grown TFs and VFSCs. The ability of these cells to adhere to fibronectin and laminin surfaces was tested. Our results summarized in Fig. 5B confirm that growing the cells on laminin rather than fibronectin caused no statistically significant effect on the fibronectin affinity. This outcome was confirmed in six replicate experiments.

3. Discussion

The dynamic communication between cells and surrounding ECM components impacts a diverse array of cellular processes

including cell adhesion, fate-restriction, migration, proliferation and survival. ECM can also play a role in the modulation of the cellular response to various cytokines and growth factors and can regulate embryonic development, tissue remodeling and repair. ECM regulates many activities of the cell such as cell adhesion, proliferation, differentiation, migration, polarity, tumorigenesis, and cancer metastasis (Jaster, 2004; Han et al., 2004). Moreover, the ECM of the vocal folds plays an important role in the biomechanics of voice production and is essential in maintaining appropriate vocal fold viscoelasticity required for phonation. The ECM is composed of fibrous proteins, structural glycoproteins, glycoaminoglycans, proteoglycans, and other interstitial molecules such as carbohydrates and lipids (Gray et al., 1999a; Labat-Robert et al., 1990). The gelatinous interstitial glyco-matrix consists of structural glycoproteins, proteoglycans, and glycosaminoglycans located in the spaces between fibrous proteins and may bind fibrous proteins influencing fiber mechanics (Pawlak et al., 1996). Additionally, interstitial proteins control tissue viscosity, water content, tissue size and thickness, and the size and density of collagen fibers (Gray, 2000; Gray et al., 1999c).

The vocal fold LP can be subdivided into three layers each with different mechanical properties: the superficial, intermediate, and deep (Hirano, 1977; Hirano et al., 1981). Immediately basal to the vocal fold epithelia and apical to the superficial layer of the LP is a transitional area called the basement membrane zone (BMZ). The BMZ contains a number of unique protein and non-protein structures important in securing the basal cells to the ECM of the superficial layer of the LP. The BMZ also helps shape the underlying LP. The influence of BMZ components on mesenchymal cells and ECM of the LP is not well understood. However, disruption of BMZ anchoring fibrils has been implicated in vocal fold nodules and other benign pathological lesions of the vocal folds (Courey et al., 1996). Basal to the BMZ is the superficial LP or Reinke's space. This layer provides a pliant cushion for the vocal fold during phonation. It is composed primarily of loose fibrous and elastic ECM with interspersed fibroblasts. The intermediate LP is the next layer of the vocal fold and adds elastic mechanical integrity to the structure. It is composed mostly of elastin fibers with scattered fibroblasts. Next, is the deep layer of the LP, which is composed almost entirely of collagen fibers and a few fibroblast cells. This layer provides durability and is ideal for absorbing tension due to its unique fiber orientation. The intermediate and deep layers of the LP comprise the vocal ligament.

A hierarchical assembly of cell-matrix adhesion complexes has been described in which these initial integrin-contacts mature to form early FX (focal complexes) and then late FX (Zaidel-Bar et al., 2004). The transformation of late FX into early FA (focal adhesions) requires a stimulus of transmembrane mechanical force, and Rho-activated kinase is central in the development of FA. Finally, mature FA and FB (fibrillar adhesions) are formed. This maturation of cell adhesion is accompanied by specific changes in the characteristic molecular components of each form of adhesion. In the early FX the first molecules observed are $\alpha\text{v}\beta\text{3}$ integrin and phosphotyrosine, followed closely by talin and paxillin. In the later stages of FX

formation vinculin, α -actinin, FAK and VASP are observed. Zyxin is recruited to the membrane during the formation of FA, and the concomitant assembly of an actin bundle occurs. FB differ from classical FA in their submembrane plaque composition and their primary integrin receptors are $\alpha\text{5}\beta\text{1}$. It has also been shown that the assembly of FB depends on the pliability of the ECM.

The vocal fold ECM is an exceptional matrix critical in maintaining the biomechanical properties of the vocal cords requisite for vibration and phonation. The ECM of the vocal folds is composed of glycosaminoglycans, structural proteoglycans and fibrous proteins distributed throughout the vocal fold LP in an organized manner optimized to tolerate the vibrational stresses associated with vocal cord vibration. Previously, the role of this complex ECM on cellular functions of fibroblasts and stellate cells found in discrete regions of the vocal fold mucosa was largely unknown. We have investigated the differences in VFSC and TF adhesion to constituents of the vocal fold ECM.

Our data demonstrate that enzymatically untreated VFSCs and TFs adhere distinctly to the various vocal fold ECM components tested. While both cell types demonstrated preferential adhesion to fibronectin, the VFSCs adhered significantly better at earlier time points. Activated hepatic stellate cells are known to enhance production and deposition of fibronectin and collagen (Kato et al., 2001; Han et al., 2004). The TFs adhered significantly better than the VFSCs to collagen type III. This may explain why VFSCs are found at the anterior and posterior ends of the vocal ligament whereas fibroblasts are able to adhere throughout the collagen type III rich regions of the vocal folds. The VFSCs exhibited significantly better adhesion to an uncoated surface than did the TFs. Hepatic and pancreatic stellate cells adhere and grow in a culture-activated manner on untreated polystyrene surfaces. The increased adhesion of these stellate cells to an uncoated surface may play a role in this phenomenon as was observed in VFSCs. Surprisingly, the VFSCs adhered significantly less well to collagen type IV, decorin, and laminin than an uncoated surface at nearly every time point tested. Decorin is known to bind collagen and delay fibril formation. Given the fibrogenic character of activated stellate cells, decorin may also prevent fibril formation by inhibiting stellate cell attachment. Laminin and collagen type IV are found predominately in the BMZ. The reduced ability of VFSCs to adhere to these components may prevent inappropriate VFSC adhesion to the BMZ where they could adversely affect the integrity of the vocal fold epithelium. Over the entire time course studied (5 to 120 min), the TFs exhibited a significant increase in adhesion to all of the ECM components tested except laminin. The VFSCs displayed greater discrimination between the ECM components to which they would adhere. Over the same time, the VFSCs demonstrated a statistically significant increase in adhesion to fibronectin, elastin and an uncoated surface. This preference may explain why the VFSCs are found predominantly in the elastin and fibronectin rich macula flava.

The pericellular HA coat is important in the earliest stages of cell adhesion. To test the role of this coat on VFSC and TF adhesion, we treated both cell types with hyaluronidase and

examined the effect this had on early adhesion up to 15 min. This treatment affected the TFs more significantly than the VFSCs and exerted the smallest effect on cell adhesion to fibronectin. Interestingly, the VFSCs treated with hyaluronidase adhered better at very early time points to an uncoated surface than to any other ECM constituent except fibronectin. This result suggests that the pericellular HA coat of the VFSCs is not entirely responsible for the preferential adhesion of these cells to an uncoated polystyrene surface. In fact, with the restoration of the HA coat at early adhesion time points, the preference of VFSC adherence to an uncoated surface is diminished. The precise receptors or mechanisms responsible for this preference remain unknown. It has been confirmed that cells possessing a prominent HA coat adhere less well to an HA treated surface than to an uncoated surface (Cho et al., 2004). In agreement with this observation, the VFSCs lacking an HA coat adhered better to the HA coated surface. We hypothesize, however, that with increasing incubation time the cells begin to produce HA causing the reduced adhesion to the HA coated surface.

The low molecular weight GTPase RhoA promotes the assembly of focal adhesions and plays a key role in cytoskeletal organization. The serine/threonine protein kinase p160ROCK is a direct target of RhoA mediated formation and assembly of stress fibers and focal adhesions (Iwamoto et al., 2000). Activation of RhoA is important in the later stages of cell adhesion (Zaidel-Bar et al., 2004). To test the role of p160ROCK on the later stages of VFSC and TF adhesion, we treated these cells with the p160ROCK-specific inhibitor Y-27632 and examined its effect on adhesion at 20 to 120 min. As with the hyaluronidase treatment, the VFSCs were more resistant to the effects of Y-27632 than the TFs. The treatment did, however, decrease the number of adherent VFSCs on every surface tested compared to the untreated VFSCs. The statically significant increase in the number of untreated adherent VFSCs from 20 to 120 min was absolved in the VFSCs treated with Y-27632 over those same time points for every surface tested. Therefore, we conclude that RhoA mediated focal adhesions play a role in VFSC and TF adhesion to vocal fold ECM components. However, since VFSC adhesion was not as affected by this treatment as TF adhesion, VFSCs may possess an alternate RhoA independent mechanism of focal adhesion maturation that may work in concert with the RhoA dependent mechanisms which appear to be critical in TF adhesion.

To investigate the observed fibronectin affinity, we: 1) grew the cells on laminin rather than fibronectin prior to testing adhesion, and 2) treated the cells with Nimesulide to inhibit the integrin $\alpha 5\beta 1$ and $\alpha v\beta 3$ mediated adhesion to fibronectin (Milliano and Luxon, 2003; Han and Roman, 2005). Growth on laminin prior to testing caused no significant change in the cells' affinity for fibronectin over laminin. Nimesulide is a COX-2 inhibitor and hepatic stellate cells produce high amounts of COX-2 during fibrogenic activation (Wang et al., 2004). The role of COX-2 upregulation in VFSC activation is unknown. Our data demonstrate that Nimesulide treatment did reduce the adhesion of the VFSCs and TFs to fibronectin coated surfaces. This suggests that the fibronectin integrin receptors $\alpha 5\beta 1$ and $\alpha v\beta 3$ likely

play a role in the increased affinity of both cell types for fibronectin coated surfaces. The reduction of cell adhesion to fibronectin may be increased with prolonged exposure to Nimesulide or these data may implicate an alternative mechanism of cell adhesion not disrupted by the Nimesulide treatment. Our results also confirm that the ability of the VFSCs and TFs to adhere to elastin coated surfaces was greatly reduced following Nimesulide treatment. Force bearing interactions between cells and elastic fibers are known to interact via integrin-dependent and independent mechanisms (Spofford and Chilian, 2003). Fibulin-5 (also known as EVEC/DANCE) is a calcium-dependent ECM protein which has been shown to bind elastin, localize to the surface of elastic fibers in vivo, and is essential in elastic fiber formation (Nakamura et al., 2002, 1999). Interestingly, fibulin-5 possesses an RGD motif recognized by many integrins, particularly $\alpha 5\beta 1$ and $\alpha v\beta 3$ integrins, through which it is thought to link elastic fibers to cell surface integrins (Yanagisawa et al., 2002). Nimesulide treatment of VFSCs and TFs may disrupt this interaction by inhibiting $\alpha 5\beta 1$ and $\alpha v\beta 3$ integrins causing the reported decrease in Nimesulide-treated cell adhesion to elastin.

This study establishes the importance of vocal fold ECM composition on the fundamental function of cell adhesion. Our results suggest a rationale for cellular distribution throughout the vocal folds based on ECM adhesion preferences. Our data also demonstrate differences between VFSCs and TFs in their capacity to adhere to various ECM materials and that this interaction is dynamic over a range of 5 to 120 min of exposure. The interaction between vocal fold cells and surrounding ECM plays an important role in a number of vocal fold pathologies as well as scarring and tissue repair (Hirano et al., 2004). It is known that activated stellate cells of the liver and pancreas promote fibrogenesis, and we hypothesize that VFSCs play a similar role in the vocal folds (Ellenrieder et al., 2004). Vocal fold scarring is a significant clinical complication of direct trauma, radiation therapy and surgery. Future experiments will begin to investigate the intercellular signaling between the VFSCs and laryngeal fibroblasts and how ECM composition and long-term exposure affect cytokine signaling, motility and response to vocal fold injury and scarring. Knowledge of the dynamic interaction between vocal fold cells and the surrounding ECM will greatly contribute to the understanding of normal laryngeal development, pathologies and the development of distinct cellular and ECM targets for future therapies.

4. Experimental procedures

4.1. Cell culture

VFSCs and TFs were collected and isolated as previously described by our laboratory with appropriate IRB and IACUC review (Fuja et al., 2006). Our laboratory has previously characterized VFSCs and demonstrated evidence that they are distinct from porcine laryngeal fibroblasts and tracheal fibroblasts. In addition, we have confirmed by careful expression and

cell morphology studies that no differences were detected between human TFs and porcine laryngeal fibroblasts (Fuja et al., 2005). In this study human TF data is reported but was found to be identical to porcine laryngeal fibroblasts (data not shown). As human VFSCs have not been isolated, we cannot make a comparison between porcine VFSCs and human VFSCs at this time. Both VFSCs and TFs were cultured on fibronectin (5 µg/ml) or laminin (5 µg/ml) at 37 °C in Dulbecco's modified Eagle medium (DMEM), high glucose with glutamine, 10% heat inactivated fetal bovine serum (FBS), 1% non-essential amino acid, 100 U/ml penicillin, 100 µg/ml streptomycin, 2.5 µg/ml amphotericin B, and 50 µg/ml gentamycin (Gibco, Carlsbad, CA) in a 5% CO₂ atmosphere.

4.2. ECM substrates

The ability of VFSCs and TFs to adhere to eight of the most prevalent naturally occurring ECM substrates found in the human vocal fold mucosa was tested. These substrates included: fibronectin, laminin, collagen types I, III, IV, elastin, decorin, and HA. Standard culture surfaces were coated with 100 µl of each of these ECM components individually at 5 µg/ml. Surface coatings were prepared at least 1 h prior to cell seeding. As a control, the ability of VFSCs and TFs to adhere to uncoated plastic surfaces was also tested.

4.3. Non-enzymatic suspension of VFSCs and TFs

To minimize potential enzymatic digestion of cell adhesion receptors during cell dissociation of adherent VFSCs and TFs prior to experimentation, cells were grown to 60% confluence and lifted using an Enzyme Free Cell Dissociation Solution (Specialty Media/Invitrogen, Carlsbad, CA). Next the cells were washed twice in PBS and re-suspended in PBS supplemented with 10 mM glucose and 0.1% bovine serum albumin (BSA). The concentration of viable cells excluding trypan blue (J.T. Baker; Phillipsburg, NJ) was determined using an improved Neubauer Bright-line hemacytometer (Hausser Scientific; Horsham, PA).

4.4. Hyaluronidase treatment

Hyaluronidase (Hyaluronidase VI-S from bovine testes; Sigma; St. Louis, MO) was added to the suspended cells to a final concentration of 200 U/ml and incubated for 60 min at 37 °C with occasional shaking. After the treatment, the cells were centrifuged, washed once in PBS and re-suspended in PBS containing 10 mM glucose and 0.1% BSA.

4.5. p160ROCK inhibitor treatment

Suspended VFSCs and TFs were treated with 25 µM (+)-(R)-trans-4-(1-aminoethyl)-N-(4-Pyridyl) cyclohexanecarboxamide dihydrochloride (Y-27632; Sigma; St. Louis, MO) for 30 min at 37 °C. Following treatment cells were washed once in PBS then re-suspended in a 10 mM glucose; 0.1% BSA; PBS solution.

4.6. Nimesulide treatment

N-(4-nitro-2-phenoxyphenyl)-methanesulfonamide (Nimesulide; Axxora; San Diego, CA) at 250 µM was introduced to cultured VFSCs and TFs for 30 min at 37 °C. These treated cells were then washed once in PBS and re-suspended in a 10 mM glucose; 0.1% BSA; PBS solution.

4.7. Fluorescence cell adhesion assay

The treated and untreated suspensions of VFSCs and TFs were then incubated with 5 µM calcein acetoxymethyl ester which is not fluorescent until it is cleaved by endogenous esterases in live cells. 1×10^5 calcein treated cells were then seeded directly into a single ECM-coated microplate well and incubated at 37 °C in a 5% CO₂ environment for 5, 10, 15, 20, 30 or 120 min. For all adhesion experiments the Corning® 96-well clear bottom black polystyrene tissue culture-treated micro assay plates were used. The tissue culture treatment of these wells was a corona discharge process which generates high energetic oxygen ion grafts on the polystyrene surface resulting in a hydrophilic, negatively charged surface. This surface was taken as the uncoated surface control in every experiment. The microplate wells were then washed three times with PBS and finally inverted for 5 min after which 200 µl PBS was added to each well prior to analysis using a FLUORstar Optima automated multi-detection microplate reader (BMG Labtech; Durham, NC). The microplate reader detected the cleaved calcein which has an absorbance maximum of 494 nm and emission maximum of 517 nm. Serial dilution and calibration was carried out to confirm a linear relationship between the number of seeded VFSCs and TFs and the relative calcein fluorescence over the range of 1×10^5 to 10 cells (data not shown). For each condition the following controls were included: PBS blank, PBS with VFSCs or TFs without calcein, serial dilution of calcein treated VFSCs or TFs from 1×10^5 to 10 cells. As a control, an aliquot of treated and untreated cells from each experiment was incubated with SYTOX Dead Cell Stain (Molecular Probes; Eugene, OR) to confirm that experimental procedures were tolerated by the cells (data not shown). The resulting fluorescence data were collected and analyzed using FLUORstar OPTIMA Analysis Software prior to statistical analysis.

4.8. Fluorescence confocal microscopy

VFSCs and TFs were grown for 72 h on each of the eight ECM surfaces. Cells were then acetone fixed at -20 °C for 20 min and the F-actin cytoskeleton was fluorescently labeled using TRITC-phalloidin (Molecular Probes; Eugene, OR). The cells were imaged using a Bio-Rad Radiance 2100 MP Multiphoton/Confocal Microscope with a 20× dry objective and a 543 nm Green HeNe Laser. Images were collected using LaserSharp2000 image analysis software (Bio-Rad Microscience Division; Cambridge, MA). Raw data were processed using Image J processing software (Research Services Branch,

National Institute of Mental Health; Bethesda, Maryland, USA) (Rasband, 2005; Abramoff et al., 2004).

4.9. Statistical analysis

Analysis of variance was used to compare adherence of the VFSCs to TFs on a given ECM substrate. Variance was also used to compare the adherence of the VFSCs or TFs to an uncoated surface compared to a specific ECM substrate at a given time interval. In addition, the variance in adhesion of the particular cell type to a specific ECM coating was also analyzed over the several time points tested. Statistical significance at a 95% confidence interval was calculated using an unpaired two-tailed *t*-test, and $p < 0.05$ was taken as significant. Data are expressed graphically in the figures as the mean \pm standard error mean (s.e.m., $n = 4$ using 5×10^4 cells per well).

Acknowledgements

This research was supported by grants from the NIDCD/NIH (grant numbers R01DC004347 and R01DC004224). We thank the University of Iowa Central Microscopy Research Facility, the Cell Fluorescence Core Facility, Iowa VA Medical Center and express profound appreciation to Dr. Gerene Denning (Research Scientist, Department of Emergency Medicine, University of Iowa) for extending her expertise.

References

- Abramoff, M.D., Magelhaes, P.J., Ram, S.J., 2004. Image Processing with ImageJ. *Biophotonics International*, pp. 36–42.
- Burgstaller, G., Gimona, M., 2004. Actin cytoskeleton remodelling via local inhibition of contractility at discrete microdomains. *J. Cell Sci.* 117, 223–231.
- Cho, M.K., Lee, G.H., Park, E.Y., Kim, S.G., 2004. Hyaluronic acid inhibits adhesion of hepatic stellate cells in spite of its stimulation of DNA synthesis. *Tissue Cell* 36, 293–305.
- Courey, M.S., Shohet, J.A., Scott, M.A., Ossoff, R.H., 1996. Immunohistochemical characterization of benign laryngeal lesions. *Ann. Otol. Rhinol. Laryngol.* 105, 525–531.
- Danen, E.H., Sonneveld, P., Brakebusch, C., Fassler, R., Sonnenberg, A., 2002. The fibronectin-binding integrins $\alpha 5\beta 1$ and $\alpha v\beta 3$ differentially modulate RhoA-GTP loading, organization of cell matrix adhesions, and fibronectin fibrillogenesis. *J. Cell Biol.* 159, 1071–1086.
- Ellenrieder, V., Schneiderhan, W., Bachem, M., Adler, G., 2004. Fibrogenesis in the pancreas. *Rocz. Akad. Med. Białymst.* 49 (40–46), 40–46.
- Fuja, T., Probst-Fuja, M., Titze, I., 2005. Transdifferentiation of vocal-fold stellate cells and all-*trans* retinol-induced deactivation. *Cell Tissue Res.* 322, 417–424.
- Fuja, T., Probst-Fuja, M., Titze, I., 2006. Changes in expression of extracellular matrix genes, fibrogenic factors and actin cytoskeletal organization in retinol treated and untreated vocal fold stellate cells. *Matrix Biol.* 25, 59–67.
- Geerts, A., 2004. On the origin of stellate cells: mesodermal, endodermal or neuro-ectodermal? *J. Hepatol.* 40, 331–334.
- Gray, S.D., 2000. Cellular physiology of the vocal folds. *Otolaryngol. Clin. North Am.* 33, 679–698.
- Gray, S.D., Hirano, M., Sato, K., 1993. Molecular and cellular structure of vocal fold tissue. In: Titze, I.R. (Ed.), *Vocal Fold Physiology: Frontiers in Basic Science*. Singular Publishing Group, San Diego, CA, pp. 1–36.
- Gray, S.D., Titze, I.R., Alipour, F., Hammond, T.H., 2000. Biomechanical and histologic observations of vocal fold fibrous proteins. *Ann. Otol. Rhinol. Laryngol.* 109, 77–85.
- Gray, S.D., Titze, I.R., Chan, R., Hammond, T.H., 1999a. Vocal fold proteoglycans and their influence on biomechanics. *Laryngoscope* 109, 845–854.
- Gray, S.D., Titze, I.R., Chan, R., Hammond, T.H., 1999b. Vocal fold proteoglycans and their influence on biomechanics. *Laryngoscope* 109, 845–854.
- Gray, S.D., Titze, I.R., Chan, R., Hammond, T.H., 1999c. Vocal fold proteoglycans and their influence on biomechanics. *Laryngoscope* 109, 845–854.
- Han, S., Roman, J., 2005. COX-2 inhibitors suppress integrin $\alpha 5$ expression in human lung carcinoma cells through activation of Erk: Involvement of Sp1 and AP-1 sites. *Int. J. Cancer*.
- Han, Y.P., Zhou, L., Wang, J., Xiong, S., Garner, W.L., French, S.W., Tsukamoto, H., 2004. Essential role of matrix metalloproteinases in interleukin-1-induced myofibroblastic activation of hepatic stellate cell in collagen. *J. Biol. Chem.* 279, 4820–4828.
- Hirano, M., 1977. Structure and vibratory behavior of the vocal folds. In: Sawashima, M., Cooper, F. (Eds.), *Dynamic Aspects of Speech Production*. University of Tokyo Press, Tokyo, pp. 13–30.
- Hirano, M., Kurita, S., Nakashima, T., 1981. The structure of the vocal folds. In: Stevens, K.N., Hirano, M. (Eds.), *Vocal Fold Physiology*. University of Tokyo Press, Tokyo, pp. 33–43.
- Hirano, S., Bless, D.M., Nagai, H., Rousseau, B., Welham, N.V., Montequin, D.W., Ford, C.N., 2004. Growth factor therapy for vocal fold scarring in a canine model. *Ann. Otol. Rhinol. Laryngol.* 113, 777–785.
- Ikeda, H., Nagashima, K., Yanase, M., Tomiya, T., Arai, M., Inoue, Y., Tejima, K., Nishikawa, T., Omata, M., Kimura, S., Fujiwara, K., 2003. Involvement of Rho/Rho kinase pathway in regulation of apoptosis in rat hepatic stellate cells. *Am. J. Physiol. Gastrointest. Liver Physiol.* 285, G880–G886.
- Iwamoto, H., Nakamura, M., Tada, S., Sugimoto, R., Enjoji, M., Nawata, H., 2000. A p160ROCK-specific inhibitor, Y-27632, attenuates rat hepatic stellate cell growth. *J. Hepatol.* 32, 762–770.
- Jaster, R., 2004. Molecular regulation of pancreatic stellate cell function. *Mol. Cancer* 3, 26.
- Kato, R., Kamiya, S., Ueki, M., Yajima, H., Ishii, T., Nakamura, H., Katayama, T., Fukai, F., 2001. The fibronectin-derived antiadhesive peptides suppress the myofibroblastic conversion of rat hepatic stellate cells. *Exp. Cell Res.* 265, 54–63.
- Kawada, N., Seki, S., Kuroki, T., Kaneda, K., 1999. ROCK inhibitor Y-27632 attenuates stellate cell contraction and portal pressure increase induced by endothelin-1. *Biochem. Biophys. Res. Commun.* 20 (266), 296–300.
- Labat-Robert, J., Bihari-Varga, M., Robert, L., 1990. Extracellular matrix. *FEBS Lett.* 268, 386–393.
- Masamune, A., Kikuta, K., Satoh, M., Satoh, K., Shimosegawa, T., 2003. Rho kinase inhibitors block activation of pancreatic stellate cells. *Br. J. Pharmacol.* 140, 1292–1302.
- Milliano, M.T., Luxon, B.A., 2003. Initial signaling of the fibronectin receptor ($\alpha 5\beta 1$ integrin) in hepatic stellate cells is independent of tyrosine phosphorylation. *J. Hepatol.* 39, 32–37.
- Murata, T., Arai, S., Nakamura, T., Mori, A., Kaido, T., Furuyama, H., Furumoto, K., Nakao, T., Isobe, N., Imamura, M., 2001. Inhibitory effect of Y-27632, a ROCK inhibitor, on progression of rat liver fibrosis in association with inactivation of hepatic stellate cells. *J. Hepatol.* 35, 474–481.
- Nakamura, T., Lozano, P.R., Ikeda, Y., Iwanaga, Y., Hinek, A., Minamisawa, S., Cheng, C.F., Kobuke, K., Dalton, N., Takada, Y., Tashiro, K., Ross, J.J., Honjo, T., Chien, K.R., 2002. Fibulin-5/DANCE is essential for elastogenesis in vivo. *Nature* 415, 171–175.
- Nakamura, T., Ruiz-Lozano, P., Lindner, V., Yabe, D., Taniwaki, M., Furukawa, Y., Kobuke, K., Tashiro, K., Lu, Z., Andon, N.L., Schaub, R., Matsumori, A., Sasayama, S., Chien, K.R., Honjo, T., 1999. DANCE, a novel secreted RGD protein expressed in developing, atherosclerotic, and balloon-injured arteries. *J. Biol. Chem.* 274, 22476–22483.

- Pawlak, A.S., Hammond, T., Hammond, E., Gray, S.D., 1996. Immunocytochemical study of proteoglycans in vocal folds. *Ann. Otol. Rhinol. Laryngol.* 105, 6–11.
- Rasband, W.S. ImageJ, U.S. National Institutes of Health. 2005. Ref Type: Computer Program.
- Sato, K., Hirano, M., 1995. Histologic investigation of the macula flava of the human vocal fold. *Ann. Otol. Rhinol. Laryngol.* 104, 138–143.
- Sato, K., Hirano, M., Nakashima, T., 2003a. 3D structure of the macula flava in the human vocal fold. *Acta Otolaryngol.* 123, 269–273.
- Sato, M., Suzuki, S., Senoo, H., 2003b. Hepatic stellate cells: unique characteristics in cell biology and phenotype. *Cell Struct. Funct.* 28, 105–112.
- Spofford, C.M., Chilian, W.M., 2003. Mechanotransduction via the elastin-laminin receptor (ELR) in resistance arteries. *J. Biomech.* 36, 645–652.
- Titze, I.R., Hunter, E.J., 2004. Normal vibration frequencies of the vocal ligament. *J. Acoust. Soc. Am.* 115, 2264–2269.
- Wang, Y.Q., Luk, J.M., Ikeda, K., Man, K., Chu, A.C., Kaneda, K., Fan, S.T., 2004. Regulatory role of vHL/HIF-1alpha in hypoxia-induced VEGF production in hepatic stellate cells. *Biochem. Biophys. Res. Commun.* 317, 358–362.
- Yanagisawa, H., Davis, E.C., Starcher, B.C., Ouchi, T., Yanagisawa, M., Richardson, J.A., Olson, E.N., 2002. Fibulin-5 is an elastin-binding protein essential for elastic fibre development in vivo. *Nature* 415, 168–171.
- Zaidel-Bar, R., Cohen, M., Addadi, L., Geiger, B., 2004. Hierarchical assembly of cell-matrix adhesion complexes. *Biochem. Soc. Trans.* 32, 416–420.
- Zimmerman, E., Geiger, B., Addadi, L., 2002. Initial stages of cell-matrix adhesion can be mediated and modulated by cell-surface hyaluronan. *Biophys. J.* 82, 1848–1857.